Kicker Magnet System of the RCS in J-PARC

J. Kamiya, T. Takayanagi, *JAERI/J-PARC, Tokai, Naka, Ibaraki, Japan*
T. Kawakubo, S. Murasugi, E. Nakamura, *KEK/J-PARC, Oho, Tsukuba, Ibaraki, Japan*

***Abstract*—Kicker magnets are installed in the extraction section of the RCS (Rapid Cycling Synchrotron) in J-PARC (Japan Proton Accelerator Research Complex) facility. They extract a 3GeV proton beam and inject it into a downstream beam transport line at a repetition rate of 25 Hz. The power supply is mainly composed of the charging unit, the pulse forming network, and thyratrons as switching device. The maximum charging voltage is 80kV. Kicker magnet is a distributed twin-C type. The circuit parameters are designed to have the 10 Ω characteristic impedance. The magnets are installed in vacuum chambers to prevent discharge. In order to accept 1 MW beam power, strict conditions are imposed on the kicker system. In the first part of this paper, we give an outline of the RCS extraction kicker system. Next, we report the specifications and performance of the power source and magnet. In addition, we report the measurements of the vacuum performance and magnetic field.**

***Index Terms*— J-PARC, RCS, kicker magnet, thyratron, vacuum**

I. Introduction

Kicker magnets are installed in the extraction section of the RCS (Rapid Cycling Synchrotron) in J-PARC (Japan Proton Accelerator Research Complex) facility. They extract a 3GeV proton beam and inject it into a downstream beam transport line. Fig.1 shows the equipment layout of the extraction section. Eight magnets are installed in two vacuum chambers, which contain three (KA1-3) and five (KB1-5) sets of magnets, respectively. As shown in Table I, there are three kinds of kicker magnets (S, M, L), distinguished by the difference in the size of their apertures. Magnetic field and kicker angle are also shown in Table I. The magnetic field is about 0.037 to 0.048T. The effective length is 0.63m per

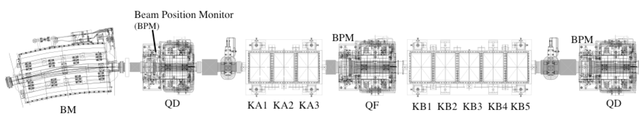

Fig. 1. Equipment layout of the extraction section of the RCS.

magnet. There are three septum magnets downstream of the kicker magnets. The integrated magnetic field of the kicker and septum magnets is 3.901 Tm in total, where the extraction angle

TABLE I
Type, Magnetic Field and Kick Angle of Kicker Magnets

	KA1	KA2	KA3	KB1	KB2	KB3	KB4	KB5
Type	L	M	S	S	S	M	L	L
By[gauss]	370	430	480	480	480	430	370	370
angle[rmad]	1.82	2.10	2.37	2.37	2.37	2.10	1.82	1.82

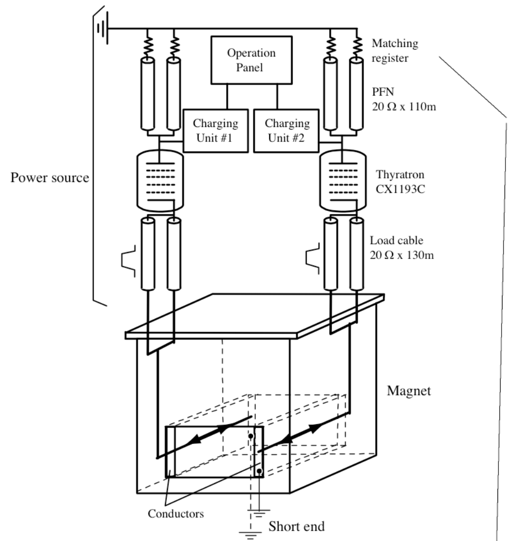

Fig. 2. Conceptual diagram of a kicker magnet system.

Resistor

is 305.67 mrad.

Fig. 2 shows the conceptual diagram of a kicker magnet system. There are eight sets of kicker magnet systems in the RCS. A kicker magnet system consists of a power source and a magnet. As shown in Fig. 2, two identical units constitute one power source. Each unit is comprised of a charging unit, PFN (Pulse Forming Network), matching registers, a thyratron switching device, and load cables. The magnet has the twin C typed shape, which means C ferrite cores are facing each other.

The charge and discharge are operated by the trigger control. When the charging trigger is input, the charging units start to charge the PFN up to the set value. The discharging trigger energizes thyratrons and then current goes through the load co-axial cables to the magnet. The currents through the conductors are reflected at the short end of the magnet. The inverse current is consumed by the matching registers in the power source.

Junichiro Kamiya, Japan Atomic Energy Research Institute, Tokai Research Establishment, 2-4 Shirane, Tokai-mura, Naka-gun, Ibaraki-ken, 319-1195 (e-mail: kamiya@linac.tokai.jaeri.go.jp).

TABLE II
SPECIFICATIONS OF A KICKER POWER SOURCE

Power Source	
Numbers	8
Output pulse shape	Rectangle
Maximum repetition rate	25Hz
PFN	Co-axial cable (~110m) [FHVCX-80, Fujikura, Ltd]
Switching device	Thyratron [CX1193C, e2V
Load cable	technologies, Ltd]
Maximum charging voltage	Same as PFN (~133m)
Maximum exciting current	80kV
Characteristic	8000A
impedance(designed value)	10Ω

The left hand and right hand side don't line up

The characteristic impedances of the components, i.e. matching registers, PFN (Pulse Forming Network), thyratron setting, load cable, and magnet, are designed to have the same value, to avoid the reflection of the current due to the impedance mismatching.

II. POWER SOURCE

Specifications of the kicker power source are summarized in Table II. The kicker power sources are produced by IDX, Ltd [1]. As described above, one power source contains two power supply units. Each unit consists of a charging unit, PFN, thyratron, load co-axial cables, and matching registers. The maximum voltage of 80 kV can be charged in the PFN, which consists of parallel co-axial cables FHVCX-80 from Fujikura, Ltd [2]. Measurement result by a LCR meter showed that the characteristic impedance of the co-axial cable is 20.2 Ω.

The charge and discharge are operated by the trigger control. Fig. 3 shows the pattern of the charging voltage. The normal repetition rate is 25 pulses per second. When the charging

I think you could delete figure 3 and say in above that charging time is 25 ms and stays charged for 15 ms before triggering.

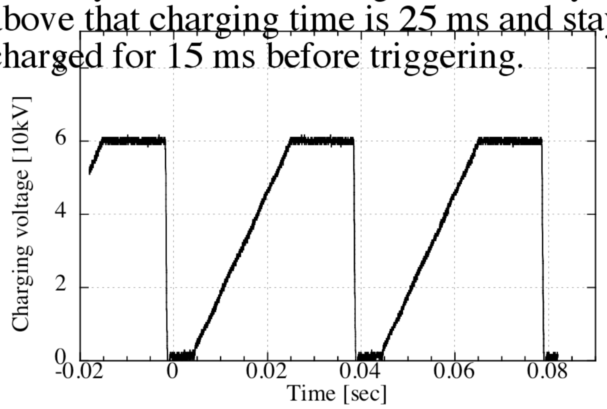

Fig. 3. Pattern of the charging voltage when the preset value is 60 kV at a repetition rate of 25 pulses per second

trigger is input, the charging units start to charge the PFN up to the set value. Then, the discharging trigger energizes thyratrons and current goes through the load cables, which are the same co-axial cable as the PFN.

As a switching device thyratron, CX1193C produced by e2V technologies, Ltd [3] is used. Thyratrons are used in very severe circumstances; that is, high peak current, high peak

Do you mean shift instead of day?A shift is a work period

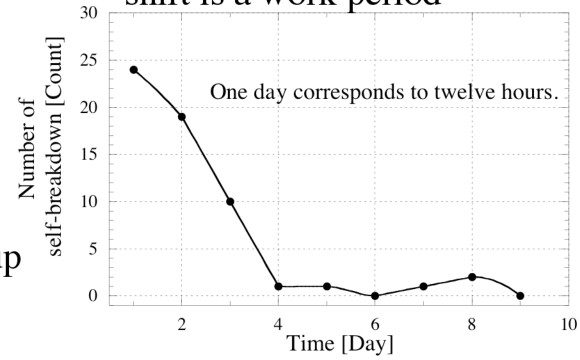

Fig. 4. Number of self-breakdowns through an aging process.

voltage, and high repetition rate. Therefore, some self-breakdown without discharge trigger occurred in operation with a new thyratron. The problem was solved by performing an aging run. The method of aging run is as follows. The charging voltage is set to start at a low level about 50 kV. Then, it is increased gradually up to 80kV over ten hours. Then, the run is continued at 70-80 kV, long enough for self-breakdown to be suppressed. Fig. 4 shows the process by which the number of self-breakdowns decreases through the aging run. The number of self-breakdowns can be reduced by an aging process of about four days.

This is a little unclear. After 10 hours do you run for 2 more hours then start at 50 kV again? And then slowly bring the voltage back up?

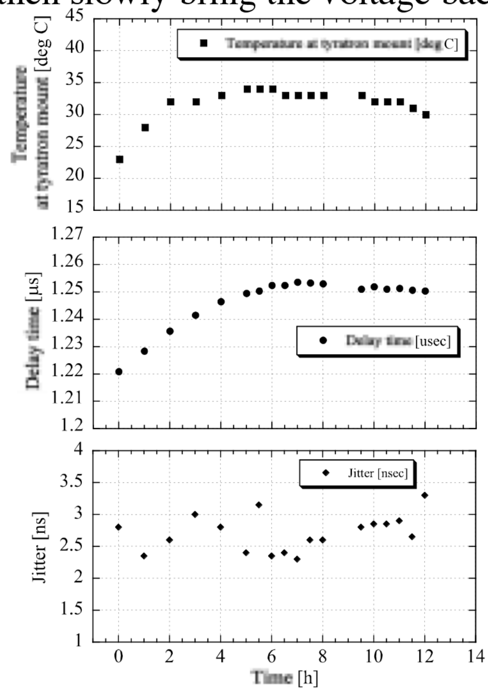

Fig. 5. Time dependence of each parameter of the power source. Each panel shows temperature of the thyratron mount, delay time, and jitter, respectively.

A thyratron mount is filled with silicon oil which cycled to cool thyratrons. The oil temperature has an effect on the characteristics of a thyratron, because pressure of the inner deuteron gas depends on the cooling oil temperature. Therefore, it is important to investigate after how much time the oil temperature stabilizes and how the temperature is related to each parameter of the power source. Fig. 5 shows the time dependence of temperature at a thyratoron mount (upper panel), delay time (middle panel), and jitter (lower panel) for 12 hours after starting to energize the power source. The exterior wall temperature of a thyratron mount was measured instead of measuring the temperature of silicon oil directly. Delay time means the time from input of a discharge trigger to a thyratron until the load current starts to flow. The lower panel shows the timing jitter of 5000 pulses. Temperature went up for 2 hours, and then it became stable. It took 6 hours for delay time to stabilize. Thus, in starting operation, consideration of the time before stable delay time is attained is required. Jitter was not affected by the temperature. There is about 2-3.5 ns jitter,

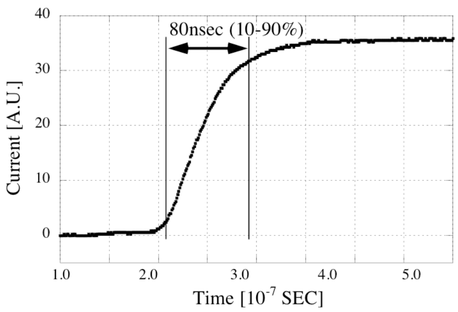

Fig. 6. Rise time of the output current measured by the current transfer installed in the shorted end of the load cable.

which is within the allowable range. Fig.6 shows the output signal from the current transfer which was installed in the shorted end of the load cable. The current rise time of the power source without the magnet was about 80nsec (10-90%).

III. Magnet

Specifications of the kicker magnet are summarized in Table III. The vacuum chambers in which magnets are installed are also described in Table III. The kicker magnets and chambers are produced by NEC/TOKIN, Ltd [4].There are three types of magnets, S, M, L, corresponding to their aperture sizes as listed in Table I. Fig. 7 shows a complete kicker magnet and a conceptual figure of its core and electrode plate. A magnet mainly consists of ferrite core (Ni-Zn), aluminum alloy (A5052), and ceramic (Al_2O_3). Aluminum alloy is used for the high voltage plates, earth plates, and conductors for exciting current. There are some ceramic parts, which are used for insulation. Ferrites are put together into C cores facing each other, the so-called twin-C type. The ferrite core is inserted between aluminium high voltage plates, and an earth plate is also inserted between them. These parts form one unit of a distributed-parameter line and twenty units constitute one magnet. The designed values of capacitance C and inductance L are 300 pF and 30 nH per unit, respectively. Thus, the characteristic impedance Z of the magnet, which is decided by the square root of L/C, is designed to be 10 Ω. However, measurement by a LCR meter at 1 kHz showed that the

TABLE III
Specifications of Kicker Magnets and Vacuum Chambers

Magnet		
Numbers		8
Characteristic impedance		10 Ω
Dimension	Vertical	960 mm
	Horizontal	776mm
	Length	638mm
Aperture size	Vertical	153 mm(S), 173 mm(M), 199mm(L)
	Horizontal	280 mm
	Length	630 mm
Magnet core		Ferrite [PE14, TDK ltd.]
Unit number		20 units/magnet
Vacuum Chamber		
Numbers		2 (A, B)
Dimension	Vertical	885 mm (A, B)
	Horizontal	1080 mm (A, B)
	Length	2495 mm (A), 4065 mm (B)

This figure might be more readable if the picture was removed?

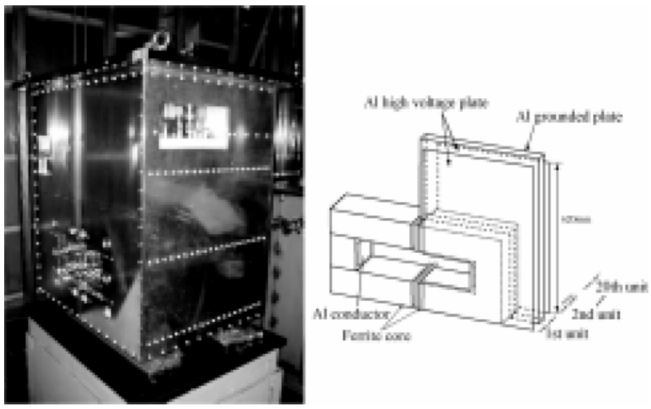

Fig. 7. Photo of a kicker magnet and conceptual figure of its cores and electrode plates.

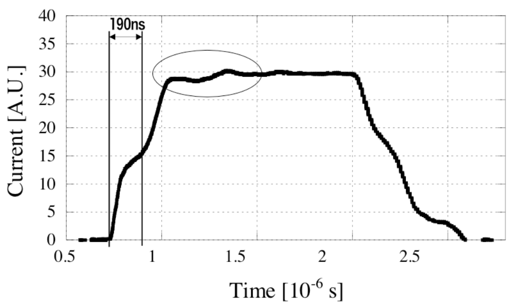

Fig. 8. Current at the entrance into the magnet with exciting only one side of the twin C type core.

It would be interesting to say something about the high voltage feedthough you use for the magnet. Does it have an inductance of less than 30 nH? Do you compensate for this inductance? It would be nice to have a much bigger graph for Fig 6 and 8 and put real units of amps on the vertical scale.

Can you show a detail of the top of the waveform in addition to the overall picture?It would be nice to change horizontal scale so that 0 sec was start of rising time

characteristic impedance of the magnet was larger than 10 Ω by 10 to 20 %. Fig. 8 shows measured current at the entrance into the magnet, provided only one side of the twin C type core is excited. The flattop just after rising edge is distorted due to the impedance mismatching between the load cable and magnet. As described before, the final high voltage plate is grounded to an earth plate, and exciting current becomes double. It should be noted that this is the superposed forward and reflected current. The time difference between a rise point and a bump caused by superposition is about 190 ns, which corresponds to a round-trip propagation time of exciting current in the magnet.

IV. VACUUM

Outgas from magnet components has large effect on vacuum and eventually on the beam itself. Especially, the outgas reduction of aluminum alloy and ferrite core is very important because they have the large surface areas 35 m^2 and 5 m^2 per one magnet, respectively. The surface of the aluminum alloy is finished by pit-free electropolishing [5]. It is reported that the processing can attain average roughness of 0.03 μm or less. These also are baked at 150 deg C for about 70 hours in a vacuum before assembling a magnet. Fig. 9 shows the effect of the baking on the outgas from aluminum alloy. The result of

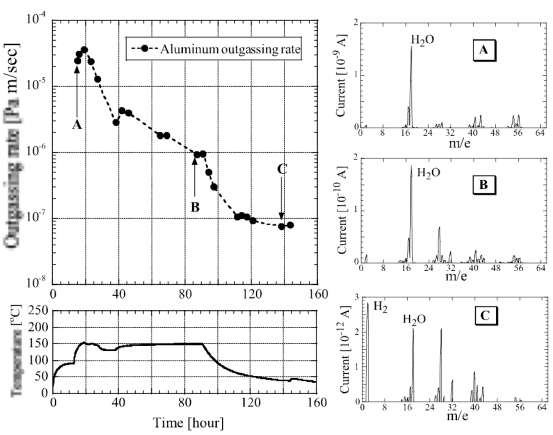

Fig. 9. Result of the outgas reduction from aluminum alloy. Each panels shows the outgassing rate (upper left), baking temperature (lower left), and mass spectrum of outgas from the aluminum alloy at each point A, B, and C in upper left panel.

mass analysis shows that the main ingredient of outgas is water. Ferrite cores are also baked in a vacuum at 200deg C for about 200 hours before assemble. The outgassing rate of each component is reduced by two or three order of magnitude. The magnets are assembled in a clean room of Class 10000.

Magnets are installed in two vacuum chambers to prevent them from discharging high voltage. Dimensions of each vacuum chamber are listed in Table III. The chambers are made from SUS304. Reduction of the outgas from the inner surface of the chamber is performed by baking at 180 deg C. The results of the build up test showed that the outgassing rate was 2.4e-8 Pa m/s. The amount of leak was found to be less than

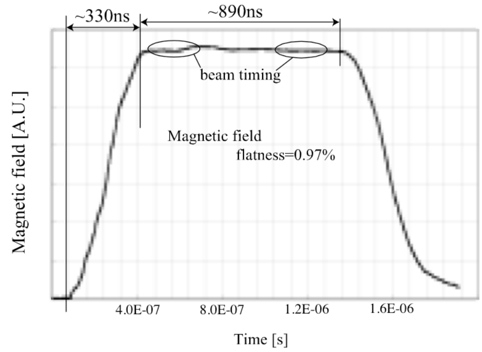

Fig. 10. Integrated magnetic field along a beam axis.

4.0e-11 Pa m^3/s by the hood method.

V. MAGNETIC FIELD MEASUREMENT

Required rise time and flattop length for the magnetic field is shorter than 350 ns and longer than 850 ns, respectively. Fig. 10 shows an integrated magnetic field along a beam axis at a charging voltage of 20 kV. The rise time and flat top length were within the requested specifications. Distribution of the integrated magnetic field is requested to have ±1% flatness. Several improvements have been performed in order to achieve the requested values [6]. We will measure the magnetic field at the rated charging voltage in a vacuum in the near future.

VI. CONCLUSION

The specifications of the extraction kicker system in the J-PARC RCS facility have been reported comprehensively. Our kicker system is required to achieve the strict requests in order to extract the large beam power of 1MW. Although there are many difficulties to manufacture this system, technical improvements have been made from the viewpoints of the power source, magnet, and a vacuum and so on.

ACKNOWLEDGMENT

We gratefully acknowledge the support of all J-PARC accelerator staff members during this project. We are especially grateful to Dr. Y. Irie and Dr. M. Kinsho for his critical reading of the manuscript.

REFERENCES

[1] IDX Corporation, http://www.idx-net.co.jp/.
[2] Fujikura Ltd., http://www.fujikura.co.jp/.
[3] e2V technologies, http://e2vtechnologies.com/.
[4] NEC/TOKIN Corporation, http://www.nec-tokin.com/.
[5] K. Tajiri, Y. Saito, Y. Yamagata, and Z. Kabeya, Journal of Vacuum Science & Technology A, A16(3), May/June 1998, pp.1196-1200
[6] J. Kamiya, T. Ueno, and T. Takayanagi, "Magnetic field measurement of the extraction kicker magnet in J-PARC RCS," submitted for publication.